Anisotropy

DOI: 10.1002/anie.200700629

Large Anisotropy and Effect of Deuteration on Permittivity in an Olefin Copper(I) Complex**

Qiong Ye, Hong Zhao, Zhi-Rong Qu, Da-Wei Fu, Ren-Gen Xiong, Yi-Ping Cui,* Tomoyuki Akutagawa,* Philip Wai Hong Chan, and Takayoshi Nakamura**

Anisotropic properties are widely exploited in many high-technology fields such as polarized-lighted microscopy, quartz wedges for determining birefringence and optical sign, liquid crystals in large displays (LCDs),[1a] thermal conductivity in microelectronic devices of solid-state transducers, and pyroelectrics in infrared detectors. Artificial dielectric resonators with anisotropic characteristics have also received much attention owing the needs of the electronics industry for materials with such properties.[1b] In general, large anisotropic effects on dielectric permittivity are only known to occur with a phase transition and disappear outside of the phase-transition-temperature range.[1c] An excellent illustration of such behavior is given by Horiuchi et al., who reported the dielectric properties of co-crystals of phenazine (phz), chloranilic acid (H_2ca), and bromanilic acid (H_2ba) along two different axes to display a huge anisotropic anomaly approximately 11 times larger than that along a third axis.[2a–d] More recently, Kobayashi and co-workers described the occurance of anisotropy of permittivity in the metal–organic framework (MOF) $[Mn_3(HCOO)_6(C_2H_5OH)]$ that was three to five times larger than that along another axis and than in the guest-free framework $[Mn_3(HCOO)_6]$, which exhibited essentially only isotropic permittivity.[3] However, these large anisotropic effects only take place near the phase transition temperature and either disappear or remain isotropic beyond this temperature. In addition, examples of anisotropic effects on temperature[4] and permittivity have been limited to systems displaying active hydrogen exchange with deuterium (for OH–OD exchange systems) that were strongly temperature-dependent. Thus, the development of large temperature-independent anisotropy and isotope effects on permittivity is an important and significant challenge.[5]

Recently, the nature of the σ-and π-bonding components of the bond between an olefin moiety and a copper(I) atom has been reported to result in their coordination not being very stable. This lability leads the resultant copper π complex to be easily polarized by an external electric field. Such a copper π complex may then display a larger molecular polarizability (χ) and thus also a larger dielectric response ($\varepsilon = 1+4\pi\chi$; ε = dielectric permittivity; in addition, the dielectric constant abides by the Debye equation: $(\varepsilon-1)/(\varepsilon+2) = N_A(\alpha_e+\alpha_d+\mu^2/3kT)/3\varepsilon_0$; α_e = electronic polarizability, α_d = molecular deformation polarizability, μ = molecular dipole moment) than normal coordination compounds.[5c,d] In this context, we envisioned a new building-block ligand that would bind to a Cu^I atom to create novel, discrete, neutral macrocyclic molecules, as shown in Scheme 1. Single crystal permittivity measurements of these new complexes showed that the dielectric constant of the partially deuterated compound displayed significant enhancement along the three crystallographic axes with a permanent and stable anisotropy and a temperature-independent increase in permittivity to more than twice that of its non-deuterated counterpart. Moreover, the anisotropy of dielectric permittivity in the deuterated and non-deuterated complexes along the three different axes (*a*, *b*, and *c*) showed huge differences, with a large permanent and stable anisotropy and an independent increase in permittivity by a factor of more than 20. To our knowledge, this is the first example of metal complexes showing such large anisotropy at high frequency (1 MHz).[2]

As shown in Scheme 1, the ligand 2-(*N*-allylpyridinium-3-yl)-1*H*-benzo[*d*]imidazole bromide (L^1) reacted with CuCl under methanolothermal conditions at 70 °C to give neutral macrocycle **1**. Under similar conditions, partially deuterated ligand 2-(*N*-allyl-2,6-dideuteriumpyridinium-3-yl)-1*H*-benzo[*d*]-imidazole bromide (L^2) also reacted with CuCl to afford neutral macrocyclic complex **2**.

X-ray single crystal structure determination of macrocyclic **1** reveals that L^1 acts as bidentate spacer that links two Cu(I) centers through the N atom of the imidazole group and

---

[*] Dr. Q. Ye, Dr. H. Zhao, Dr. Z.-R. Qu, D.-W. Fu, Prof. Dr. R.-G. Xiong, Prof. Dr. Y.-P. Cui
Ordered Matter Science Research Center and
School of Electronic Science and Engineering
Southeast University
Nanjing, 211189 (China)
Fax: (+86) 25-5209-0626
E-mail: xiongrg@seu.edu.cn
ypcyp@seu.edu.cn

Prof. Dr. T. Akutagawa, Prof. Dr. T. Nakamura
Research Institute for Electric Science
Hokkaido University
Sapporo 060-0812 (Japan)
Fax: (+81) 11-706-497
E-mail: takuta@es.hokudai.ac.jp
tnaka@imd.es.hokudai.ac.jp

Prof. Dr. P. W. H. Chan
Division of Chemistry and Biological Chemistry
School of Physical and Mathematical Sciences
Nanyang Technological University
Singapore 637616 (Singapore)

[**] This work is supported by 973 (2006CB806104), the National Natural Science Foundations of China Nos.(20471029, 20490214 and 50673039). X.R.G. thanks Nanjing University for supporting the synthesis and characterization of the ligands and complexes used in this work. P.W.H.C. thanks Nanyang Technological University for funding.

Supporting information for this article is available on the WWW under http://www.angewandte.org or from the author.

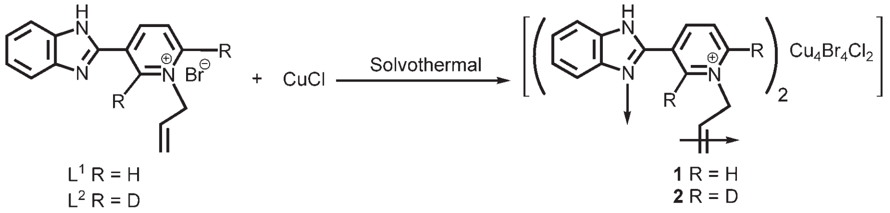

Scheme 1.

the olefin moiety. This arrangement results in the formation of a large neutral molecular macrocycle with a 22-membered ring along the bond sequence Cu2A-Br2A-Cu1A-N1A-C7A-C8A-C12A-N3A-C13A-C14A-Cu2-Br2-Cu1-N1-C7-C8-C12-N3-C13-C14, as shown in Figure 1 a.[6] The space-filling diagram depicted in Figure S1 in the Supporting Information reveals that there is no free cavity to accommodate guest molecules. This assessment is further supported by elemental analysis and thermogravimetric analysis, which indicate that no guests or absorbed molecule persists in the cavity before the decomposition temperature (see the Supporting Information Figure S11). There are two crystallographically independent Cu atoms, each of which displays a distorted trigonal coordination geometry formed by a N atom from the imidazole unit, a μ_2-Br atom, and a terminal Br atom for the Cu1 center, and by a terminal Cl ligand, a μ_2-Br atom, and the olefin moiety of the allylic group for the Cu2 center. The Cu−Cu distance is about 2.871 Å, thus indicating there is weak interaction between the two Cu atoms. Inspection of Figure 1 b, which shows a packing view of **1**, reveals formation of a three-dimensional polymer through weak supramolecular interaction with H····Br distances of 2.910 Å.

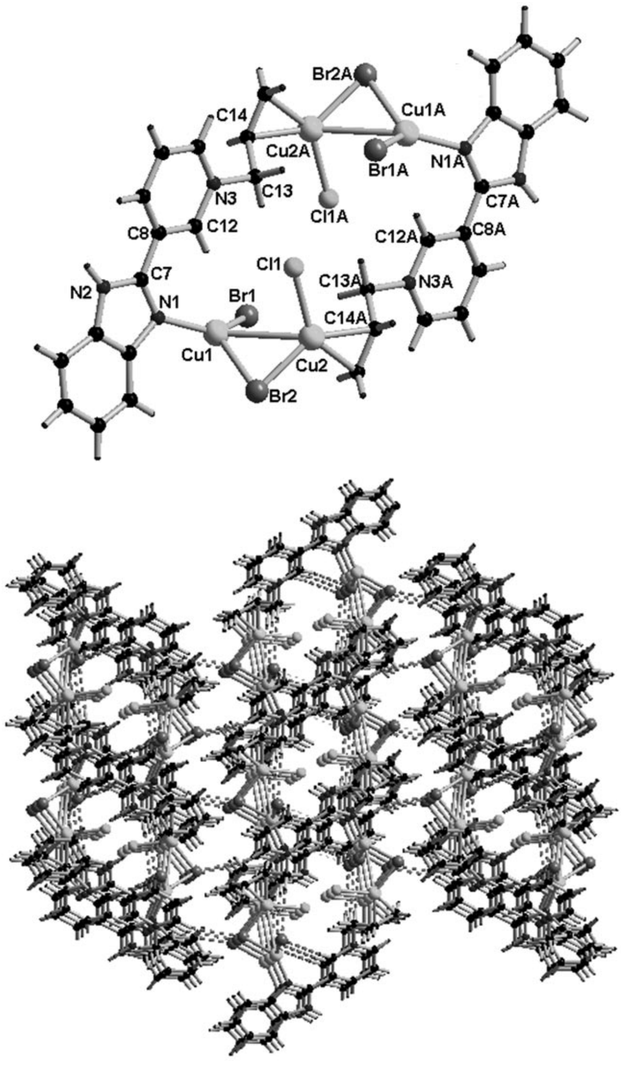

Figure 1. a) Crystal structure of **1** in which four Cu atoms and two L^1 ligands form a 22-membered ring and all of the Cu atoms display distorted trigonal geometry. b) Packing view of **1** revealing a pseudo-three-dimensional polymer through weak supramolecular interactions along the *c* axis with H····Br distances (dotted lines) of 2.910 Å.

As anticipated, macrocycle **2** consists of a 22-membered ring along the bonding sequence Cu2A-Br2A-Cu1A-N1A-C7A-C8A-C12A-N3A-C13A-C14A-Cu2-Br2-Cu1-N1-C7-C8-C12-N3-C13-C14 (Figure 2 a), since it is isostructural to **1**.[6] The weak supramolecular interactions with D····Br distances of 2.804 Å are stronger than those of macrocycle **1**, which suggests that the anisotropy along the *c* axis may be quite different on going from **1** to **2** (Figure 2 b). There are no abnormal C−C, C−N, C=C, Cu−N, Cu−Cl, or Cu−Br bond lengths in either **1** or **2**. The $Cu-C_{olefin}$ bond lengths (2.028–2.083 Å for **1** and 2.058–2.066 Å for **2**) are also in good agreement with those previously reported for Cu olefin complexes.[7]

The temperature dependence of the alternating current (ac) permittivity was investigated. Measurements of single crystals **1** and **2** were carried out on an impedance analyzer between 5 and 300 K and from 10^3 to 10^6 Hz. Electrical contacts were prepared using gold paste to attach the 10-μm diameter gold wires to the single crystals. The permittivity of a single crystal of **1** along three crystallographic axes ($E \parallel c$, $E \parallel a$, $E \parallel b$ for the electric field approximately parallel to *c*, *a*, and *b* axis, respectively; Figure 3) reveals that the permittivity remains essentially unchanged over the entire temperature range and from $10^{4.5}$ to 10^6 Hz, reaching values of 640, 71, and 28 for $E \parallel c$, $E \parallel a$, and $E \parallel b$, respectively (see Figures S2–S4 in the Supporting Information). This temperature independence resembles that of organic crystals of squaric acid derivatives (SQA) reported by Sugawara and co-workers[8] and by Moritomo et al.[9] The magnitude of the dielectric constant in a single crystal of **2** (Figure 4) along the *c* axis ($E \parallel c$) is much larger than that of **1** over the entire temperature range and reaches a value of 1392 (2.18 times the value for **1**). Nevertheless, the dielectric behavior displays a temperature independence similar to that of **1** (Figure S5). Similarly, enhancements of a factor of more than 2.4–2.5 compared to **1** (179/71 and 68/28) are also observed for the *a* and *b* axes owing to deuteration. This result is comparable to examples in the literature showing large anomalies on permittivity arising from deuteration, such as the $[Mn_3(HCOO)_6(C_2H_5OH)]/[Mn_3(HCOO)_6(C_2H_5OD)]$ system for which the

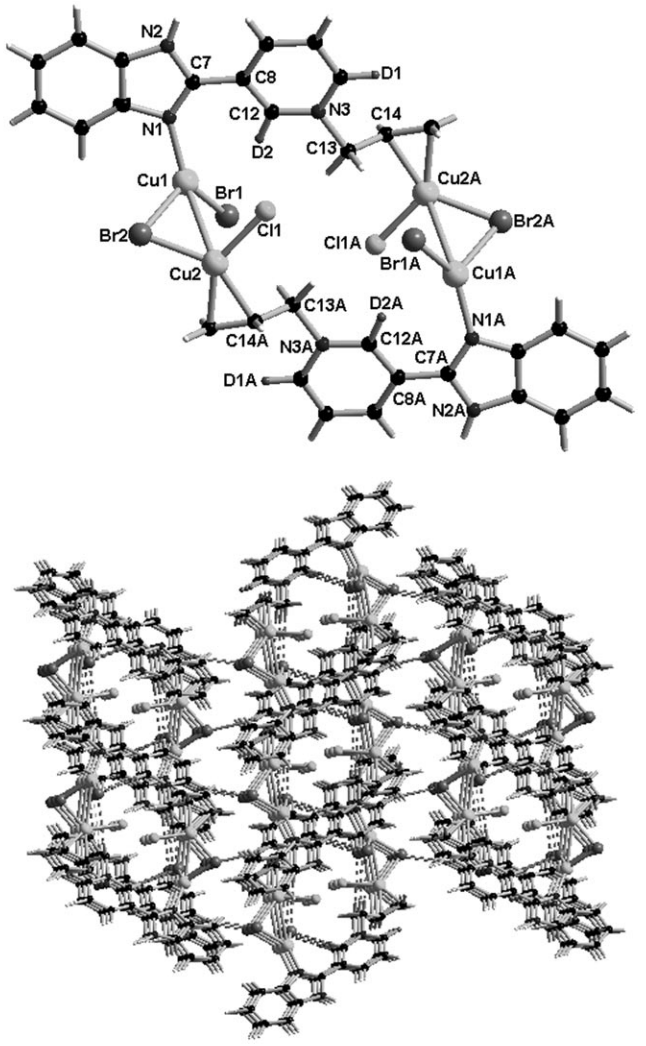

Figure 2. a) Crystal structure of **2** in which four Cu atoms and two L^2 ligands make up a 22-membered ring and all of the Cu atoms display distorted trigonal geometry. b) Packing view of **2** revealing a pseudo-three-dimensional polymer through weak supramolecular interactions along the *c* axis with a D····Br distance (dotted lines) of 2.804 Å.

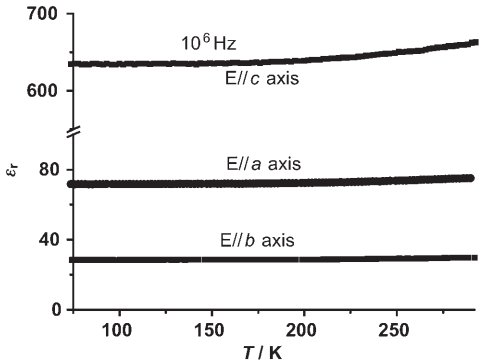

Figure 3. Temperature dependence of dielectric permittivity (ε_r) of non-deuterated **1** for the electric field $E \| c$ axis, $E \| a$ axis, and $E \| b$ axis at 1 MHz.

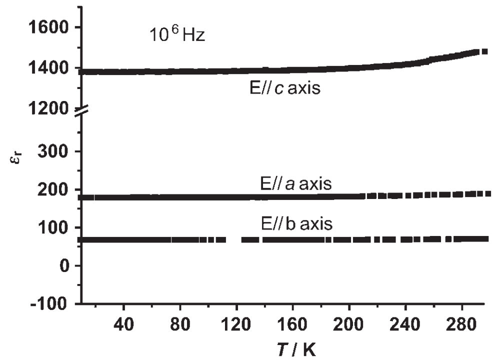

Figure 4. Temperature dependence of dielectric permittivity (ε_r) of deuterated **2** for the electric field $E \| c$ axis, $E \| a$ axis, and $E \| b$ axis at 1 MHz.

permittivity increases from 45 to 57 between a non-deuterated and a deuterated guest.[3] SQA also displays a strong isotope effect with the permittivity increasing from 9 to 18 between non-deuterated and deuterated SQA.[8]

Dynamic H-bonds may play an important role in the isotope effect on the dielectric constant in both the MOF and SQA systems, with dielectric anomalies (or peaks) rapidly disappearing with increasing temperature beyond a phase-transition region or displaying close temperature-dependent characteristics. Weak supramolecular H···Br (or D···Br) interactions in **1** and **2** may also be responsible for the large isotope effect on the dielectric constant through changes in dipole arrangements and lattice modulations of the crystals. The static supramolecular C–H···Br and C–D···Br interactions between the aromatic rings and neighboring Cu coordination environments result in a static and stable MOF lattice, for which the deuterated mass effect is constant and permanent, remaining unchanged with increasing temperature. This situation strongly suggests that the permittivity in the present case displays temperature-independent behavior.[8] Since the absolute magnitude of the dielectric constant depends on the molecular polarizability and on crystal density, deuterated C–D···Br interactions in compound **2** increase the molecular polarizability and the density of the packing structure. In fact, the much shorter D····Br interaction and larger crystal density in **2** than in **1** may also partially contribute to the occurrence of a large isotope effect on permittivity. To our knowledge, such a large, permanent, and stable effect of deuteration on permittivity ($\varepsilon_{\mathrm{r}\|\mathrm{c}}$D/$\varepsilon_{\mathrm{r}\|\mathrm{c}}$H, $\varepsilon_{\mathrm{r}\|\mathrm{a}}$D/$\varepsilon_{\mathrm{r}\|\mathrm{a}}$H and $\varepsilon_{\mathrm{r}\|\mathrm{b}}$D/$\varepsilon_{\mathrm{r}\|\mathrm{b}}$H, see Figures S6–S8 in the Supporting Information) that is also temperature-independent is unprecedented.

The temperature dependence of dielectric anisotropy of single crystals of **1** and **2** was investigated using the same single crystals as for the permittivity studies discussed above. These anisotropy measurements revealed that the dielectric behavior of **1** and **2** displayed significant anisotropy. The largest anisotropic effect on the dielectric constant between the *c* and *b* axes (defined as $\varepsilon_{\mathrm{r}\|\mathrm{c}}/\varepsilon_{\mathrm{r}\|\mathrm{b}}$, where ε_r is the real part of the complex permittivity ($\varepsilon = \varepsilon_\mathrm{r} + \mathrm{i}\,\varepsilon_\mathrm{i}$), and the subscripts $\|$c and $\|$b indicate that the electric field is parallel to the *c* and *b* axes) was observed to reach an enhancement of more than a factor of 20–22; this very large anisotropic effect resembled the anomaly found in the ternary cocrystal system phz–H_2ca–

H_2ba between the *b* and *c* axes with a dielectric-constant enhancement of approximately a factor of ten.[2] On the other hand, the dielectric anisotropy in single crystals of **1** and **2** between the *c* and *a* axis and the *a* and *b* axis ($\varepsilon_{r\|C}/\varepsilon_{r\|a}$ and $\varepsilon_{r\|a}/\varepsilon_{r\|b}$) is much lower, with increases by factors of 7.8–8.8 and 2.5–2.7, respectively (Figures 5 and 6). It is interesting to note that the temperature independence of permittivity remains constant. Such large and stable anisotropy occurring in three different crystal axes could be due to the anisotropy of molecular polarizability and molecular orientation in the crystal, which results in solid-state molecular polarity differences (see Figures S9–S10 in the Supporting Information).[1b] To our knowledge, this phenomenon in metal complexes is not known to date.

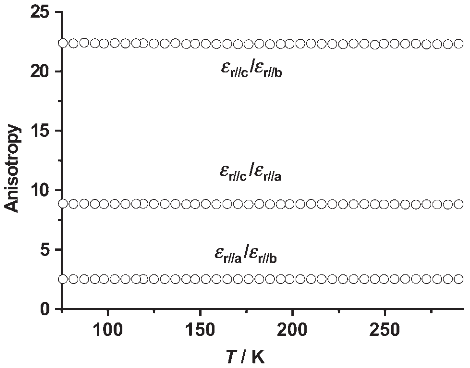

Figure 5. Anisotropies in a single crystal of **1** ($\varepsilon_{r\|c}/\varepsilon_{r\|b}$, $\varepsilon_{r\|c}/\varepsilon_{r\|a}$, and $\varepsilon_{r\|a}/\varepsilon_{r\|b}$) as a function of temperature showing temperature-independent behavior.

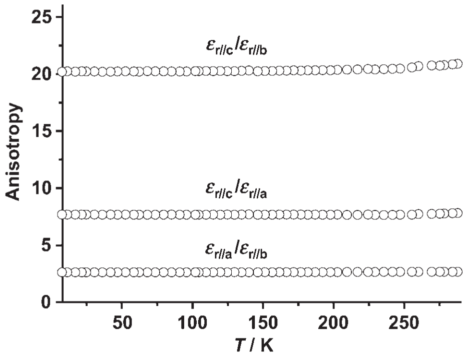

Figure 6. Anisotropies in **2** ($\varepsilon_{r\|c}/\varepsilon_{r\|b}$, $\varepsilon_{r\|c}/\varepsilon_{r\|a}$, and $\varepsilon_{r\|a}/\varepsilon_{r\|b}$) as a function of temperature showing temperature-independent behavior.

In summary, we have demonstrated that the dielectric behavior in two novel Cu^I olefin complexes with partial deuteration on the aromatic ring displays a permanent and stable isotope effect and anisotropy. It is envisioned that our findings will provide a new impetus to devising new strategies to applications in high-technology fields, such as anisotropic dielectric detectors or resonators.

Experimental Section

See the Supporting Information for experimental details on the synthesis of ligands L^1 and L^2.

1: Thermal treatment of CuCl (1 mmol) and L^1 (1 mmol) in methanol (2 mL) at 70 °C over 1–2 days gave pale yellow crystalline blocks of **1** in approximately 45 % yield based on the amount of L^1 consumed; only one pure phase was found. Elemental anal. calcd (%) for $C_{20}H_{28}Br_4Cl_2N_6Cu_4$: C 21.48, H 2.51, N 7.52; found: C 21.53, H 2.48, N 7.61; IR (KBr): $\tilde{\nu} = 3447$(s), 3104(s), 1633(m), 1594(w), 1536(w), 1498(w), 1475(s), 1438(m), 1418(m), 1386(w), 1323(m), 1281(w), 1258(w), 1225(w), 1151(m), 1135(m), 992(m), 942(w), 818(w), 795(w), 751(s), 678(s) cm^{-1}.

2: Following the same procedure as for **1** but replacing L^1 with L^2 affords **2** as pale yellow crystalline blocks in 50 % yield based on the amount of L^2 consumed. Elemental anal. calcd (%) for $C_{20}H_{24}D_4Br_4Cl_2N_6Cu_4$: C 21.31, H 2.14, N 7.49; found: C 21.47, H 2.09, N 7.38; IR (KBr): $\tilde{\nu} = 3445$ (m), 3335(m), 3054(w), 2362(w), 2305(w), 1610(m), 1577(w), 1549(w), 1494(w), 1494(w), 1424(s), 1424(w), 1337(w), 1280(m), 1228(w), 1177(w), 986(w), 938(w), 876(w), 763(s), 621(w), 575(m) cm^{-1}.

Received: February 11, 2007
Revised: April 12, 2007

Keywords: copper · deuterium · dielectric constant · isotopic effects · X-ray diffraction

---

[1] a) H. Korner, A. Shiota, T. J. Bunning, C. K. Ober, *Science* **1996**, *272*, 252; b) A. Munir, N. Hamanaga, H. Kubo, I. Awai, *IEICE Trans. Electron.* **2005**, *E88-c*, 40; c) F. C. Krebs, P. S. Larsen, J. Larsen, C. S. Jacobsen, C. Boutton, N. Thorup, *J. Am. Chem. Soc.* **1997**, *119*, 1208.

[2] a) S. Horiuchi, R. Kumai, Y. Tokura, *J. Am. Chem. Soc.* **2005**, *127*, 5010; b) S. Horiuchi, Y. Okimoto, R. Kumai, Y. Tokura, *Science* **2003**, *299*, 229; c) S. Horiuchi, R. Kumai, Y. Okimoto, *J. Am. Chem. Soc.* **1999**, *121*, 6757; d) S. Horiuchi, F. Ishii, R. Kumai, Y. Okimoto, H. Tachibana, N. Nagaosa, Y. Tokura, *Nat. Mater.* **2005**, *4*, 163; for inorganic compounds measured at 1 MHz, see: e) M. A. Subramanian, D. Li, N. Duan, B. A. Reisner, A. W. Sleight, *J. Solid State Chem.* **2000**, *151*, 323; f) H. Amorin, V. V. Shvartsman, A. L. Kholkin, M. E. Costa, *Appl. Phys. Lett.* **2004**, *85*, 5667.

[3] a) H.-B. Cui, Z. Wang, K. Takahashi, Y. Okano, H. Kobayashi, A. Kobayashi, *J. Am. Chem. Soc.* **2006**, *128*, 15074; b) H.-B. Cui, K. Takahashi, Y. Okano, H. Kobayashi, Z. Wang, A. Kobayashi, *Angew. Chem.* **2005**, *117*, 6666–6670; *Angew. Chem. Int. Ed.* **2005**, *44*, 6508–6512.

[4] T. Akutagawa, S. Takeda, T. Hasegawa, T. Nakamura, *J. Am. Chem. Soc.* **2004**, *126*, 291.

[5] a) Q. Ye, Y.-M. Song, G. X. Wang, D.-W. Fu, K. Chen, P. W. H. Chan, J.-S. Zhu, D. S. Huang, R.-G. Xiong, *J. Am. Chem. Soc.* **2006**, *128*, 6554 (highlighted in Editors' Choice section in *Science* **2006**, *312*, 974; b) T. Okubo, R. Kawajiri, T. Mitani, T. Shimoda, *J. Am. Chem. Soc.* **2005**, *127*, 17598; c) N. J. Long, *Angew. Chem.* **1995**, *107*, 826; *Angew. Chem. Int. Ed. Engl.* **1995**, *34*, 21; d) S. Barlow, H. E. Bunting, C. Ringham, J. C. Green, G. U. Bublitz, S. G. Boxer, J. W. Perry, S. R. Marder, *J. Am. Chem. Soc.* **1999**, *121*, 3715; e) D.-W. Fu, Y.-M. Song, G.-X. Wang, Q. Ye, R.-G. Xiong, T. Akutagawa, T. Nakamuna, P. W. H. Chan, S. D. Huang, *J. Am. Chem. Soc.* **2007**, *129*, 5346.

[6] Crystal data for **1**: $C_{20}H_{28}Br_4Cl_2N_6Cu_4$, $M_r = 1117.28\,g\,mol^{-1}$, monoclinic, space group $P2_1/n$, $a = 7.7471(11)$, $b = 21.762(3)$, $c = 10.2707(15)$ Å, $\beta = 103.269(2)°$, $V = 1685.3(4)$ Å^3, $Z = 2$, $\rho_{calcd} = 2.202\,Mg\,m^{-3}$, $R_1 = 0.0506$, $wR_2 = 0.1163$, $\mu = 7.424\,mm^{-1}$, $S =$

1.070. Crystal data for **2**: $C_{20}H_{24}D_4Br_4Cl_2N_6Cu_4$, $M_r = 1121.31$, monoclinic, space group $P2_1/n$, $a = 7.721(2)$, $b = 21.660(3)$, $c = 10.212(3)$ Å, $\beta = 103.307(4)°$, $V = 1661.9(8)$ Å^3, $Z = 2$, $\rho_{calcd} = 2.241$ Mg m^{-3}, $R_1 = 0.0478$, $wR_2 = 0.1022$, $\mu = 7.528$ mm^{-1}, $S = 1.082$. The structures were solved by direct methods using the program SHELXTL (Sheldrick, 1997).[10] All non-hydrogen atoms were located from the trial structure and refined anisotropically with SHELXTL using the full-matrix least-squares procedure. The hydrogen and deuterium atom positions were fixed geometrically at calculated distances and allowed to ride on the parent carbon atoms. The final difference Fourier map was found to be featureless. CCDC-631979 (**1**) and CCDC-631980 (**2**) contain the supplementary crystallographic data for this paper. These data can be obtained free of charge from The Cambridge Crystallographic Data Centre via www.ccdc.cam.ac.uk/data_request/cif.

[7] a) X.-F. Huang, Y.-M. Song, X.-S. Wang, J. Pang, J.-L. Zuo, R.-G. Xiong, *J. Organomet. Chem.* **2006**, *691*, 1065; b) Q. Ye, X.-S. Wang, H. Zhao, R.-G. Xiong, *Chem. Soc. Rev.* **2005**, *34*, 308; c) X. Xue, X.-S. Wang, R.-G. Xiong, X.-Z. You, B. F. Abrahams, C.-M. Che, H.-X. Ju, *Angew. Chem.* **2002**, *114*, 3068 – 3070; *Angew. Chem. Int. Ed.* **2002**, *41*, 2944 – 2946.

[8] I. Takasu, A. Izuka, T. Sugawara, T. Mochida, *J. Phys. Chem. B* **2004**, *108*, 5527.

[9] Y. Moritomo, Y. Tokura, H. Takahashi, N. Mori, *Phys. Rev. Lett.* **1991**, *67*, 2041.

[10] G. M. Sheldrick, SHELXTL V5.1 Software Reference Manual, Bruker AXS, Inc., Madison, Wisconsin, USA, **1997**.